ELSEVIER

Journal of Nuclear Materials 290–293 (2001) 840–844

journal of nuclear materials

www.elsevier.nl/locate/jnucmat

Analysis of energy flux deposition and sheath transmission factors during ergodic divertor operation on Tore Supra

L. Costanzo *, J.P. Gunn, T. Loarer, L. Colas, Y. Corre, Ph. Ghendrih, C. Grisolia, A. Grosman, D. Guilhem, P. Monier-Garbet, R. Reichle, H. Roche, J.C. Vallet

Association EURATOM-CEA sur la Fusion contrôlée, DRFC-SIPP, CEA Cadarache, 13108 Saint Paul Lez Durance, France

Abstract

The magnetic deflection of field lines to dedicated wall components in the ergodic divertor of Tore Supra generates complex patterns of power deposition. In this paper, we analyze the energy flux deposition on neutralizer plates as measured by infrared cameras and Langmuir probes. Three important features will be discussed: (1) The energy deposition during helium shots is as much as twice that for deuterium shots, for a given input power level. (2) The sheath heat transmission factor, deduced experimentally by comparison between probes and infrared measurements, increases with input power independently of the working gas from $\sim$7.5 ($P_{TOT} = 1$ MW) to $\sim$10–11 for $P_{TOT} = 5$ MW). In ohmic discharges, the standard value of 7 is recovered except specific cases in helium where γ can decrease to 2 or 3. (3) These anomalous values put in doubt the validity of edge temperature measurements by Langmuir probes in detached plasmas and have led to the development of a promising 'infrared' degree of detachment (Dod). © 2001 Elsevier Science B.V. All rights reserved.

Keywords: Parallel heat flux; Ergodic divertor; Plasma sheath heat transmission factor; Degree of detachment

1. Introduction

For the design of next-generation fusion devices, it is critical to estimate and to control heat loads to the objects in contact with the plasma, such as limiters and divertor neutralizer plates. In Tore Supra, the ergodic divertor configuration generates specific patterns of power deposition and allows better control of energy and particle deposition [1]. A crucial point is the dependence of heat deposition patterns on the discharge parameters (total input power, density, radiation, etc.). These parameters affect the energy flux arriving at the surface and act on the sputtering suffered by the divertor target. The magnetic configuration at the plasma edge induced by the ergodic divertor results in a significant reduction of the parallel heat flux on the target plates [1], providing the opportunity to perform discharges at high input power level. This paper concentrates on an experimental investigation of energy flux onto the target plates with a survey of the influence of additional power and a comparison between working gases (helium and deuterium). The effects of auxiliary heating on the edge density regimes are discussed in Section 2. After a description of the dedicated diagnostics used to measure the heat flux deposition, Section 3 is devoted to the study of the heat flux impinging onto the target plates. Section 4 is dedicated to the discussion of the plasma sheath heat transmission factor, with a comparison between experimental and standard modeling. Based on a simple model, an 'infrared' degree of detachment is defined providing a powerful tool with a view to characterize the considered regime (attached–detached) independently of the magnetic configuration in all divertor discharges. The resulting analysis is discussed in Section 5. Finally, in Section 6, we review the conclusions.

* Corresponding author.
E-mail address: costanzo@drfc.cad.cea.fr (L. Costanzo).

PII: S0022-3115(00)00647-4

2. Effect of auxiliary heating on edge density regimes

In the following sections, the reported results have been obtained when the resonant magnetic equilibrium was established [1] (safety factor $q_{\rm edge} \sim 3$, plasma current $I_{\rm p} = 1.45$ MA and toroidal field $B_{\rm t} = 3.2$ T). Experiments have been performed without active pumping (outboard pumped limiter position = 3.18 m, behind the front face of the divertor) in order to isolate the effect of the divertor [2]. Edge plasma parameters have been modified by using up to 4 MW of ion cyclotron resonance heating (ICRH), and by changing the working gas (helium and deuterium). Density scans are systematically considered for the reported experiments.

Fig. 1 gives the evolution of the edge density ($n_{\rm e\_edge}$) versus the volume averaged density for deuterium discharges. $n_{\rm e\_edge}$ is measured by Langmuir probes mounted on the target plates. The first two classical density regimes (sheath-limited and high recycling, [3]) are observed: a linear variation of $n_{\rm e\_edge}$ for $\langle n_{\rm e} \rangle$ lower than 2×10^{19} m^{-3} and then a nearly quadratic dependence for larger $\langle n_{\rm e} \rangle$ as schematically shown in Fig. 1. At high input power level, large sawteeth appear leading to strong oscillations of the edge density. From the resulting edge electron temperature $T_{\rm e\_edge}$, a clear shift to high averaged plasma volume density with increasing power level is observed in Fig. 2. The edge temperature is also strongly affected by sawteeth. In contrast to ohmic shots, the coupling of the ICRH wave to the edge plasma requires an attached plasma [4]. Furthermore, when the power rises, the natural operating density is higher. It should be noticed that the different shots have comparable gas puffing rates varying from 5 to 9.5 Pa m^3 s^{-1}. Similar experiments have been performed in 'pure' helium and the edge plasma ($n_{\rm e\_edge}$, $T_{\rm e\_edge}$) exhibits the same behaviors as deuterium (at higher volume averaged plasma density level).

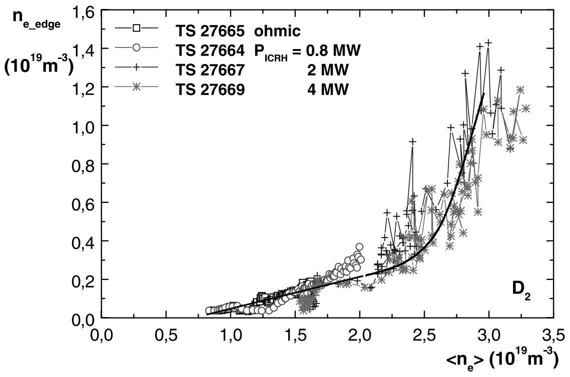

Fig. 1. Density at the neutralizer plate as a function of the volume averaged density (deuterium discharges) for different ICRH heating levels.

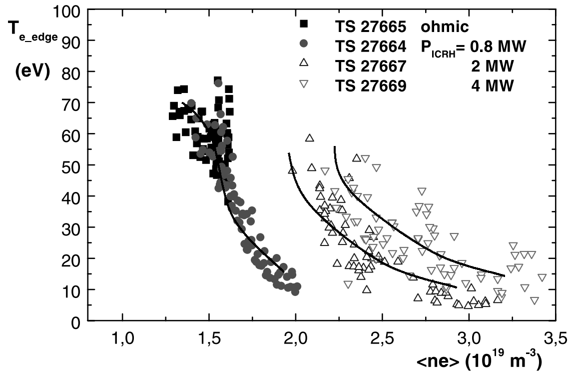

Fig. 2. Electron temperature at the neutralizer plate as a function of the volume averaged density (deuterium discharges) for different ICRH heating levels.

3. Parallel heat flux

The energy flowing to the divertor target plates can be determined by two different diagnostics on Tore Supra. Fourteen Langmuir probes are installed on the divertor plates at different poloidal and toroidal locations [5]. Thermographic measurements viewing these neutralizer plates can also be performed simultaneously using three high resolution infrared cameras located at 120° toroidal sectors. The target plates are made of copper, actively cooled and coated with boron carbide (B_4C).

The parallel heat flux at the plate deduced from probe measurements can be written as

$$Q_{//\rm Probe} = \gamma \Gamma_{//} T_{\rm e\_edge}, \tag{1}$$

where γ is the sheath heat transmission factor and $\Gamma_{//}$ is the parallel ion flux. The standard sheath theory yields $\gamma = 7$ for deuterium plasma with $T_{\rm i} = T_{\rm e}$, [3]. It is a key parameter for modeling since it determines the boundary conditions for the fluid equations. Section 4 is devoted to this quantity.

The heat flux deduced from infrared measurements can be calculated from the surface temperature

$$Q_{//\rm Infrared} = \Delta T \frac{\lambda_{\rm B_4C}}{e_{\rm B_4C}} \frac{1}{\sin\alpha}, \tag{2}$$

where ΔT is the surface temperature variation of the plate, $\lambda_{\rm B_4C}$ the thermal conductivity (1.5 W m^{-1} K^{-1}), $e_{\rm B_4C}$ the target plate B_4C coating thickness (200 μm) and α is the incidence angle between the field line and the neutralizer plate. We assume that the surface temperature responds instantly to temporal variations of incident heat flux. The time constant of the boron carbide layer is about 5 ms. The IR camera has 20 ms temporal resolution. Fig. 3 represents the evolution of the mean

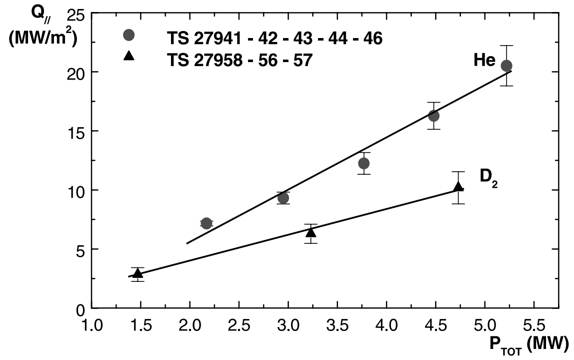

Fig. 3. Infrared mean parallel heat flux as a function of total input power for helium shots (circles) and deuterium shots (triangles).

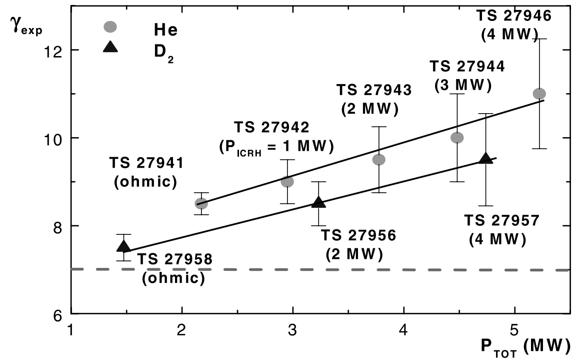

Fig. 4. Experimental heat transmission factor as a function of total input power for helium shots (circles) and deuterium shots (triangles).

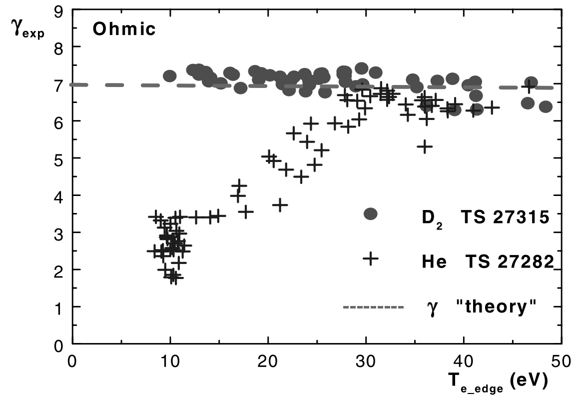

Fig. 5. Experimental heat transmission factor as a function of the edge temperature for an ohmic helium shot (cross) and an ohmic deuterium shot (circles).

heat flux (averaged value during the ICRH pulse) as a function of the total input power (P_{TOT}).

An increase is observed for both gases but it is much higher in helium than in deuterium, the mean level of the flux being larger by nearly a factor 2 over the power range. This behavior can be attributed to a better particle screening effect in deuterium which is one of the most important effects which results from the use of the ergodic divertor [6,7]. This is presumably due to the longer mean free path for helium and the different charge exchange cross-section. The neutral density is certainly different and should be taken into account. Indeed, the recycling flux, the wall particle content and the resulting outgasing are much higher in deuterium which very likely leads to a larger neutral density at the edge. Also, the radiated power greater in deuterium than in helium supports this idea. But it is difficult to estimate this power when auxiliary heating is applied [8,9]. The role of the radiation needs to be investigated further, but is beyond the scope of this paper.

4. Plasma sheath heat transmission factor

From Eq. (1), it can be seen that the sheath heat transmission factor γ plays an important role in terms of thermal exchange between ions and electrons in the sheath. This factor has been investigated under different conditions for a long time [10]. The sheath potential affects the energy flux arriving at the surface and contributes to the sputtering yield of impurities [11]. In Tore Supra, the correlation between the heat flux deduced from Langmuir probes and infrared measurements allows one to determine an experimental value of this factor

$$\gamma_{\text{exp}} = Q_{//\text{Infrared}}/\Gamma_{//}T_{\text{e\_edge}}. \qquad (3)$$

As illustrated in Fig. 4, a typical increase of γ_{exp} from $\sim$7.5 to $\sim$10–11, respectively, for $P_{TOT} \sim 1$ to 5 MW is observed with the total input power independently of the working gas. Such high values of γ_{exp} for auxiliary heated discharges can be interpreted by a T_i/T_e ratio around 2–3 as discussed later in this section.

The increase in the size of the error bars at high input power is due to sawtooth activity.

The mixed discharges (He/D_2) show similar evolutions to deuterium discharges. Nevertheless, some ohmic shots in pure helium are significantly lower than the normally accepted $\gamma = 7$ value. The involved evolution is shown on Fig. 5 where γ_{exp} is plotted as a function of $T_{\text{e\_edge}}$ for one characteristic shot in pure D_2 and one shot in pure He. While for D_2, the γ_{exp} remains close to 7 over the all $T_{\text{e\_edge}}$ range, for He, the γ_{exp} becomes as low as 2 or 3 for low edge temperature, (i.e. $T_e \sim 10$ eV). From $T_e \sim 15$ to $\sim$30 eV, a linear increase of γ_{exp} is observed while for higher temperature, $T_e \sim 30$ to 50 eV ($\langle n_e \rangle \sim 4 \times 10^{19}$ m^{-3}), the standard value of $\gamma \sim 7$ is recovered.

Such low values (~2 to 3) have already been observed on DIII-D without precise specified experimental conditions or a clear explanation [12,13]. While the high values might be expected as a result of an elevated ion temperature, values of γ below 7 are more difficult to explain [3,12]. From a theoretical point of view, the complete expression of the floating potential can be written including the contribution of the charge and the isentropic exponent μ [14,15]:

$$\psi = 0.5\ \ln\left[\left(\frac{2\pi m_e}{m_i}\right)\left(Z + \frac{\mu T_i}{T_e}\right)(1-\delta_e)^{-2}\right], \qquad (4)$$

where m_i, m_e, T_i and T_e are the ion and electron masses and temperatures, respectively. μ is a function related to the thermodynamic properties of the plasma, and is linked to the number of degrees of freedom for a given plasma species. Specific expressions are valid in different regimes of collisionality: $\mu = 5/3$ for high collisionality regime; $\mu = 3$ for the collisionless regime; $5/3 < \mu < 3$ for intermediate regimes [16]. Z is the charge and δ_e is the secondary electron emission coefficient.

Finally, the sheath heat transmission factor is

$$\gamma = 2\frac{1}{1-\delta_e} + \frac{2}{Z}\frac{T_i}{T_e} - \psi. \qquad (5)$$

Fig. 6 shows the evolutions of γ as a function of the ion/electron temperature ratio, Z and δ_e (the mass ratio has a very weak influence). The proposed theory does not lead to values as low as experimentally obtained. The lowest predicted values are to ~5 for $T_i \ll T_e$. From Fig. 6, one can see that the influence of the secondary electron emission coefficient is weak in contrast to the temperature ratio. It implies that high values of γ would correspond to a temperature ratio greater than 1 at the edge when auxiliary heating is applied in contrast to the T_i/T_e of around 1 in ohmic case. Furthermore, the behavior in helium and deuterium is not expected to be different.

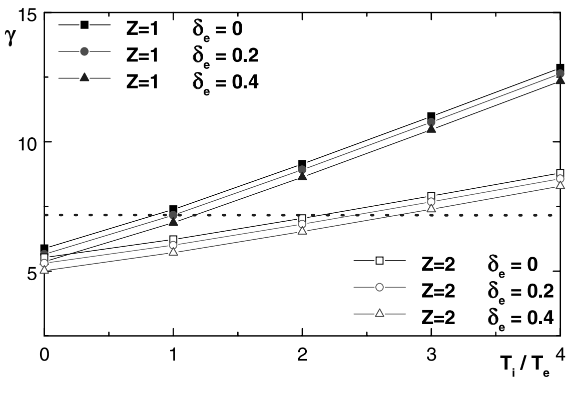

Fig. 6. Theoretical heat transmission factor as a function of T_i/T_e, Z and δ_e.

The analysis leads to different possible explanations for the low values recorded for γ_{exp}. One of these explanations could be related to an overestimation of the electron temperature given by the Langmuir probes [17]. Langmuir probe measurements are based on the assumption of a Maxwellian electron distribution. An energetic electron tail can affect the value of the sheath potential. The non-Maxwellian tail can significantly affect plasma diagnostics, parallel heat fluxes, plasma-neutral and plasma-impurities interactions. This tail of electrons can result in an overestimate of the temperature by probes by at least a factor 2 [18]. An alternative explanation is the role played by the momentum-changing collisions (elastic scattering and charge-exchange collisions) of the plasma ions with neutral gas. These collisions reduce the ion energy by transferring it to the neutral gas. Since the plasma ions arrive at the wall with lower energy, the power transmission factor is reduced [13]. However, deuterium plasmas are most collisional and cannot explain such low values [19]. The last feature would be the occurrence of two populations, helium I and helium II. A thorough study of this point is planned in the future.

5. 'Infrared' degree of detachment

Feedback algorithms using edge measurements to control the gas injection into the discharge have long played an important role in Tore Supra [20]. The density limit in deuterium discharges is preceded by detachment and a MARFE-like phenomenon. On Tore Supra, the detachment signature is usually characterized by a fall of the edge temperature below 10 eV. All the feedback algorithms discussed here define an empirical degree of detachment (Dod) [21]. Two methods of defining detachment already exist on Tore Supra: one based on local measurements obtained with the Langmuir probes [22] and one using integrated measurements from edge bolometry [23]. Technological and operational constraints on the one hand and the difficulties to determine the Dod with the probes in some cases (complex power deposition patterns as in the ergodic divertor case) on the other hand have led us to develop a third way to quantify the detachment. The model used here is based on the variation of the parallel heat flux to the plate derived from the infrared signals. Thus, this 'infrared' Dod is directly correlated to the heat flux in the same way the 'probe' Dod is correlated to the ion flux. Indeed, due to the correlation between the particle flux and the heat flux, the plasma detachment is obviously accompanied by a strong decrease of the heat flux which can be reduced to nearly zero. The procedure to calculate the heat flux deposition on the surface is based on solving the heat conduction equation. Using a numerical solution of a differential equation for 1-D heat transfer into

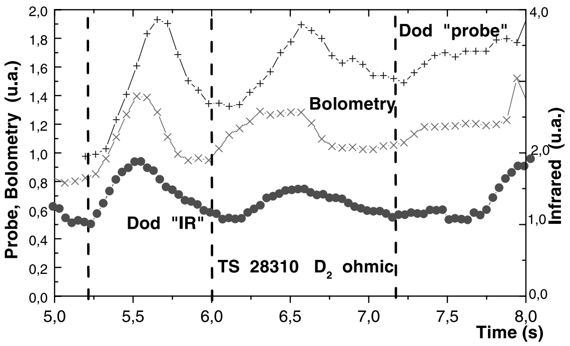

Fig. 7. Temporal evolution of the 'probe' and 'infrared' Dod and bolometry detachment criterion. Vertical dash lines symbolize the onset of the detachment phase.

a semi-infinite solid, an accurate time dependence of the heat flux deposition can be obtained. The different detachment criteria are displayed in Fig. 7 as a function of the time for a shot with a feedback control on the Dod (deduced from the probes) with the gas injection. For the attached regime, the infrared Dod remains very close to 1. At the time of detachment, the Dod increases clearly. As illustrated in the figure, the comparison between the different curves shows a quite good agreement.

It should be emphasized that this method has a major advantage in terms of spatial resolution (comparing to the very local probe measurements) especially in regard to the peaking factor of the power flux [1,24]. Finally, the infrared signals cover a wide range of temperature analysis from maximum technologically permitted temperatures to low detachment temperatures.

6. Conclusion

During ergodic divertor operation on Tore Supra, the energy deposition on the target plates is nearly twice as high in helium discharges than in deuterium discharges for a given line average density. The sheath heat transmission factor has been determined experimentally by comparing infrared heat flux measurements with probe flux and temperature measurements. A typical increase γ from $\sim$7.5 (for $P_{TOT} = 1$ MW) to $\sim$ 10–11 (for $P_{TOT} = 5$ MW) is observed with the total input power independently of the working gas. On the other hand, the standard value close to 7 is recovered most of the time in ohmic discharges as expected in usual theory except specific cases, in particular for helium ohmic shots. Finally, a very promising 'infrared' Dod has been developed. Such a useful tool will allow detachment to be controlled in terms of heat flux.

Acknowledgements

The authors wish to thank J.-Y. Pascal and S. Vartanian for providing valuable data as well as the referees for their help in improving the paper.

References

[1] Ph. Ghendrih, A. Grosman, H. Capes, Plasma Phys. Control. Fus. 38 (1996) 1653.
[2] T. Loarer, Ph. Ghendrih, J.P. Gunn et al., Particle collection and exhaust in ergodic divertor experiments on Tore Supra, these Proceedings.
[3] C.S. Pitcher, P.C. Stangeby, Plasma Phys. Control. Fus. 39 (1997) 779.
[4] F. Nguyen, A. Grosman, V. Basiuk et al., J. Nucl. Mater. 278 (2000) 117.
[5] J.P. Gunn, A. Azéroual, M. Bécoulet et al., Plasma Phys. Control. Fus. 41 (1999) B243.
[6] C. Grisolia, Ph. Ghendrih, J.P. Gunn et al., Density regime studies during ergodic divertor experiments at Tore Supra, these Proceedings.
[7] Ph. Ghendrih, Tore Supra team, Plasma Phys. Control. Fus. 39 (1997) B207.
[8] R. Reichle, J.C. Vallet, M. Chantant et al., in: 25th EPS Conference on Controlled Fusion and Plasma Physics, Prague, Czech Republic, 1998.
[9] R. Reichle, J.C. Vallet, V. Basiuk et al., in: 25th EPS Conference on Controlled Fusion and Plasma Physics, Maastricht, Netherlands, 1999.
[10] H. Kimura, H. Maeda, N. Ueda et al., Nucl. Fus. 18 (1978) 1195.
[11] J.M. Pedgley, G.M. McCracken, Plasma Phys. Control. Fus. 35 (1993) 397.
[12] P.C. Stangeby, Plasma Phys. Control. Fus. 37 (1995) 1031.
[13] A.H. Futch, G.F. Matthews, D. Buchenauer et al., J. Nucl. Mater. 196–198 (1992) 860.
[14] R. Chodura, in: D.E. Post, R. Behrisch (Eds.), Physics of Plasma–Wall Interactions in Controlled Fusion, Series B Physics, NATO ASI Series, Plenum, Que, 1984.
[15] P.C. Stangeby, Phys. Fluids 27 (11) (1984) 2699.
[16] E. Zawaideh, F. Najmabadi, R. Conn, Phys. Fluids 29 (2) (1986) 463.
[17] R.D. Monk, A. Loarte, A. Chankin et al., J. Nucl. Mater. 241–243 (1997) 396.
[18] O.V. Batischchev, S.I. Krasheninnikov, P.J. Catto et al., Phys. Plasmas 4 (5) (1997) 1673.
[19] T.Q. Hua, J.N. Brooks, Phys. Plasmas 1 (11) (1994) 3607.
[20] C. Grisolia, Ph. Ghendrih, A. Grosman et al., J. Nucl. Mater. 275 (1999) 95.
[21] A. Loarte, R. Monk, J.R. Martin-Solis et al., Nucl. Fus. 38 (1998) 331.
[22] J.P. Gunn, J. Bucalossi, L. Costanzo et al., Plasma Phys. Control. Fus. 42 (2000) 557.
[23] B. Meslin, T. Loarer, Ph. Ghendrih et al., J. Nucl. Mater. 266–269 (1999) 318.
[24] A. Grosman, Ph. Ghendrih, B. Meslin et al., J. Nucl. Mater. 241–243 (1997) 532.